ORIGINAL ARTICLE

Threshold of the skull injury for blunt force impacts under free and constraint boundary conditions

Lea Siegenthaler[1] · Michael Strehl[2] · Alessio Vaghi[1] · Philippe Zysset[3] · Beat P. Kneubuehl[4] · Martin Frenz[2]

Abstract

The formation of skull fractures is an important topic in legal medicine. In particular, the influence of boundary conditions is controversially discussed in the literature. A study focusing solely on this aspect was missing. This study aimed to investigate the influence of boundary conditions on the energy threshold for head fractures. Because of the great variability of biological tissue of real skulls, we opted for a head model made from a polyurethane sphere filled with gelatin. Furthermore, we decided to investigate two opposite situations: A fixed configuration where a model was placed on a rigid surface and a (quasi) free boundary configuration where the head model was held at a force of 5 N compensating for gravity. For both configurations, we determined the acceleration signal of the impactor, the force, and the energy threshold for head fracture. It turned out that the fracture forces for both configurations were the same whereas the energy threshold was 11.0 J for the fixed and 13.6 J for the free boundary. The difference seems to be negligible if compared to the effect of varying structural mechanical properties of real human heads. This means that in a forensic case, the two situations most probably cannot be distinguished. To investigate the influence of the impactor mass, we developed a mathematical model and fitted the experimental data. As a result, we found that in the free configuration, a larger mass increases the energy threshold for head fracture. So that in principle, the two configurations are distinguishable.

Keywords Blunt impact · Skull fractures · Energy threshold · Head model · Boundary condition

Introduction

Cases which involve blunt force impact to the head are an everyday occurrence in forensic science. Park and Son [1] showed 10% of Korean homicides are committed using blunt instruments, whereas Ambade and Godbole [2] revealed even 41% of Indian homicides involved blunt force of which 80% targeted the head. Blunt force to the head can lead to skull fractures, which are an indicator of minor brain injuries [3] and to death in more severe cases. Hence, it is important to gain a thorough understanding of the mechanisms involved by

this type of injury. A variety of studies have been performed to determine tolerance criteria and a tolerance level for skull fractures. Good overviews of the performed research can be found in Yoganandan et al. [4], Verschueren and Delye et al. [5, 6], Mole et al. [7], and Viano et al. [8].

However, only few studies examined the influence of boundary conditions with controversial results.

Kroman et al. [9] performed drop tower experiments on two female and three male unembalmed heads with an intact scalp over the impact site. They used two configurations. In the first, the skulls were fixed on a scored wooden board that broke very easily to simulate a situation with free boundary condition. In the second one, an intact wooden board was used that just bent slightly without breaking. In that way, a situation of semirigid boundary could be simulated. Fractures with free boundary conditions occurred at forces between 5396 and 6272 N lasting 1.1–3.0 ms after the impact. One head was tested in a semirigid configuration leading to a fracture force of 4559 N. Fractures occurred on the impact side for the free configuration whereas they also occurred on the opposite side for the semirigid configuration. The final results show a

✉ Lea Siegenthaler
lea.siegenthaler@irm.unibe.ch; https://www.irm.unibe.ch

[1] Institute of Forensic Medicine, University of Bern, Bern, Switzerland

[2] Institute of Applied Physics, University of Bern, Bern, Switzerland

[3] Institute for Surgical Technology and Biomechanics, University of Bern, Bern, Switzerland

[4] Bpk Consultancy GmbH, Thun, Switzerland

difference in force and in the fracture pattern between the two configurations.

Schneider et al. [10] and Nahum et al. [11] dropped an impactor on embalmed and unembalmed heads of post mortem human subjects. The heads were placed on soft rubber foam to simulate a real life situation. Preliminary tests suggested that a rigid support behind the head increases the impact force by 20–30% in comparison to a situation without support where the head can move freely.

Ruan et al. [12, 13] numerically simulated the pressure response inside a human head to side impacts. They concluded that there is no difference between the response of a freely moving head and one held by a neck force. However, in the case where the head motion is restricted fully, the pressure response changes.

Verschueren and Delye et al. [5, 6] used two pendula on the same fulcrum. On one, they fixed an embalmed head or a skull, and on the other, a flat-surfaced, aluminum cylinder of 70 mm diameter with a force sensor and a laser displacement sensor. The first pendulum had an overall mass of 9.6 kg while the second one had a mass of 14.4 kg. They concluded that no significant motion of the head occurred before fracture, implying that the boundary condition has no influence on the fracture process.

One source of the controversy could be the different boundary conditions tested. Another could be the great variability of biological tissues employed and hence, the limited experimental reproducibility. This becomes evident when considering the results presented for the parietal and frontal part of the head. Using seven human heads, Raymond et al. [14] observed a very large range for the fracture force: 3376–6347 N for an impact velocity of 20 m/s and 3547–9529 N for a velocity of 35 m/s. Mole et al. [7] also found a large range using 30 porcine heads: 4120–9110 N for an impact velocity of 18 m/s and 9080–12,800 N for 24 m/s. Schneider et al. [10] using 17 human heads, reported fracture forces between 4140 and 9880 N for the frontal bone whereas Nahum et al. [11] after 20 measurements on male and female heads reported fracture forces of 4792–8852 N and 2669–6228 N, respectively. Verschueren et al. [5, 6] found fracture forces of 6444–11,838 N for 5.21 m/s and 7311–14,269 N for 6.95 m/s. Examining these intervals and their largeness, it is evident that investigating situations with different boundary conditions is a challenging task.

In this context, we decided to investigate two opposite situations: a head placed on rigid surface and a head that moves freely after a very low force threshold is reached. To increase the experimental reproducibility, we used a very simple head model consisting of a spherical bone and brain simulant.

The goal of our study was to investigate the influence of the boundary conditions on the energy threshold for a head fracture and thereby answer whether it is possible in a forensic case to distinguish between the above two opposite situations, also relying on the severity, the shape, and the structure of the skull damage.

Materials and methods

Head model

For this study, we used head models instead of human heads because we could not get the large number of human heads required to obtain statistically relevant results. The head models consisted of a bone and a brain simulant without hair and skin. This guaranteed a high reproducibility of the experimental results. As a bone simulant, we used a polyurethane sphere with a diameter of 19 cm and a thickness of 0.7 cm coated by a rubber periosteum manufactured by Synbone AG (Malans, Switzerland). The sphere was then filled with 10% ballistic gelatin from GELITA as a soft tissue simulant leading to a head model mass of 3.32 kg (± 0.01 kg).

Such, a head model has already been tested for ballistic and blunt force impacts [15–17]. These studies showed that on a macroscopic scale, this artificial bone produces the same fracture patterns as real human bone but when examined closely, it presents slight differences in size and shape [15, 18, 19]. These slight differences in the fracture pattern were accepted in favor of the reproducibility of our experimental results. In comparison to real skulls, the head model of our study has a higher fracture force[1] but a similar force-deflection curve [20]. The head model was cooled to 4 °C and during the experiment, the temperature increased maximally to 6 °C. Cronin and Falzon [21] showed that the difference between the mechanical properties of gelatin in this temperature range can be neglected for the pressures under which we tested [12].

We have conducted preliminary tests investigating the expansion of the fractures on the head model surface. Micro-CT scans were taken and showed a rather local distribution of the cracks formed. To avoid any influence between adjacent impacts, the distance between impact sites was chosen larger than 5 cm, resulting in a high reproducibility of the measurements when hitting the same head model several times.

Setup

Two sets of experiments were performed. In the first set, the head model was placed on an aluminum bowl with a depth of 3.1 cm fixed on a wooden block. From here on, this is referred to as the fixed configuration. The second set, represents a situation with free boundary condition (Fig. 1). In this case, the head model was placed on a thin aluminum ring with a mass of 255 g with a chamfered edge. The ring perfectly fits the shape of the head model and had the same diameter as the bowl used in the fixed configuration. A rig with three adjustable magnets held the ring with the head model in such a way that a force of only 5 N, just enough to compensate for gravity,

---

[1] In comparison to real long bones (e.g., hemurus) Frankenberg et al. [18] found a lower fracture force for polyurethane cylinders.
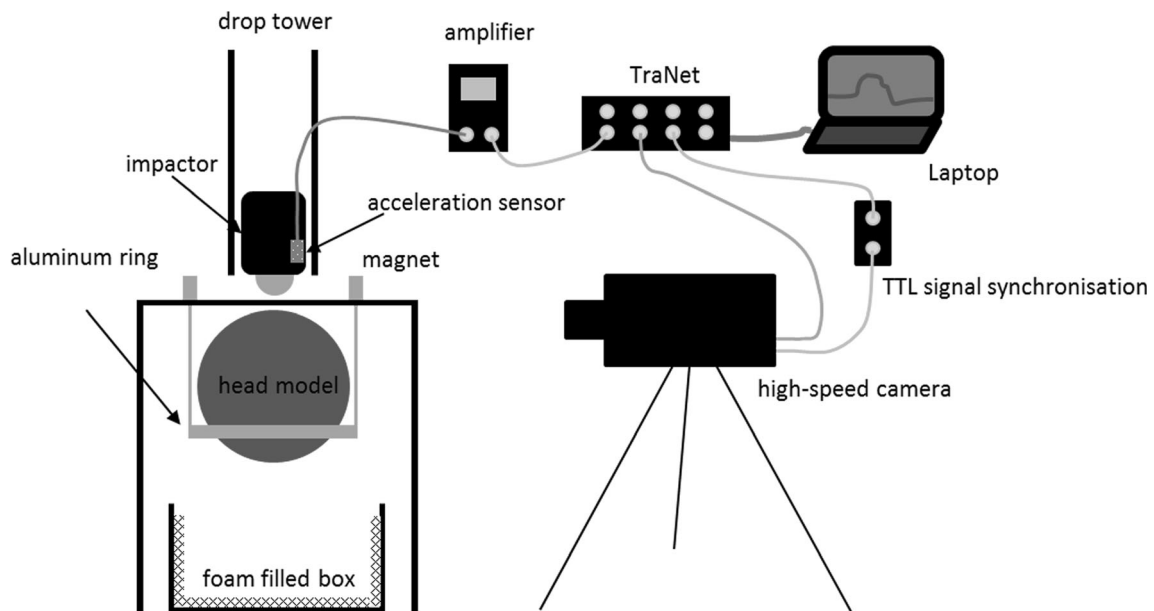
Fig. 1 Schematic setup of the free boundary configuration

was necessary to release the ring. This force threshold was measured with a press force sensor (Kistler 9313AA1) placed on the impact site and gradually increasing the pressure.

The model was hit by a cylindrical impactor with a hemispherical heading section made of hardened steel, falling from a drop tower. The impactor had a mass of (2.14 ± 0.01) kg and a diameter of 5 cm. During experiments with the fixed configuration, the impactor had to be manually stopped after the hit with the model to ensure only one impact. In the free configuration, the model fell in a box with soft rubber foam to avoid any further damage.

For all experiments, an acceleration sensor (Kistler K-Shear Accelerometer 8704B5000) was mounted on the impactor. During the pretest session, an additional accelerometer was mounted directly on the head but the signal was masked by strong and long lasting noise caused by vibrations. Therefore, we fixed the accelerometer to the aluminum ring. Both sensors were connected to an amplifier (Kistler 5015A) and the data was recorded by a TraNET FE (Elsys) transient-recorder at a sampling rate of 1 MHz.

The acceleration signals were synchronized to a high-speed camera (Photron FASTCAM SA-X2) and a LED-Booster light source. The camera recorded pictures with 400,000 fps at an exposure time of 23.4 μs.

Experimental procedure

To determine the 50% energy threshold for the fracture, the impactor has been dropped on head models from different heights, separated by intervals of 5 cm. The exact height was measured with a laser rangefinder (± 2 mm). Table 1

summarizes the heights, energies, and number of impacts for each configuration.

Each head model was impacted six times in the free as well as in the fixed configuration to have a direct comparison at a specific energy. If the space between two impact sites was sufficient, we performed additional impacts always keeping the minimum distance of 5 cm. A total of 20 head models were employed in doing so at least two head models were used for each energy level.

The head model was tracked on the video by means of ProAnalyst with an uncertainty of ± 0.04 pixel/mm. In such a way, we followed the geometrical center of the head model which corresponds to the center of mass (COM). From the video images, we measured the starting time of the head motion, the displacement, the velocity, and the energy of the head. The starting time was measured with an uncertainty of ± 75 μs.

We defined the deformation of the skull in the free configuration as the change of the distance between the

Table 1 Heights, energies, and number of impacts for the fixed and the free configuration. The height is affected by an uncertainty of ± 2 mm which corresponds to an energy uncertainty of ± 0.04 J

Height (m)	Energy (J)	#Fixed	#Free
0.50	10.50	23	12
0.55	11.55	39	18
0.60	12.60	33	39
0.65	13.65	25	48
0.70	14.70		30
0.75	15.75		14

Number of impacts

positions of the COM and the impactor (taken from video images, see the "Results" section). In the fixed configuration, we defined the deformation only accounting for the displacement of the impactor, i.e., the deformation of the whole head.

The acceleration signal was analyzed with the help of Matlab. The low signal to noise ratio forced us to apply a low-pass third-order Butterworth filter with a cut-off frequency of 600 Hz. We calculated the force signal multiplying the acceleration signal by the head mass. Fracture events were analyzed by means of the acceleration signal. We defined the starting time of a fracture as the instant when the force started decreasing while the deformation still increased. The fracture force was defined as the force measured at this time. The starting time of the contact was defined as the instant when the signal surpassed the threshold of 3 g, where g is the gravity acceleration. We calculated the absorbed energy in the fracture by integrating the force-deformation-curve up to the time of fracture.

Mathematical model

To investigate the influence of the impactor mass on the fracture, we developed a mathematical model consisting of springs (with constants k_1, k_2, k_3) and a dashpot (with damper coefficient η), see Fig. 2. Here, m_I (resp. m_H) is the mass of the impactor (resp. head) and x_1, x_2, x_3 are position displacements. For the fixed configuration the third spring was turned completely stiff (i.e. $k_3 \to \infty$) and for the free configuration, it was turned off (i.e., $k_3 = 0$). Solving the second equation of DE with respect to x_3, one can reduce the original system to two ordinary differential equations—one of the 3rd order in x_1

and the other one of 2nd order in x_2—for which we impose the following initial conditions:

$$x_1(0) = 0; \ \dot{x}_1(0) = -\sqrt{2gh}; \ \ddot{x}_1(0) = -g; \ x_2(0)$$
$$= 0; \ \dot{x}_2(0) = 0. \tag{IC}$$

Here, h is the height at which the impactor has been dropped. Note that the mathematical model only represents the total impact without fracture (or the impact up to fracture).

Using Matlab we performed a least-square fit taking filtered data of each experiment for the fixed and the free configuration, with and without fracture. As fit parameters, we chose k_1, k_2, and η. Since the mathematical model only describes the physical system up to the point of fracture, signals after the fracture were disregarded and their data were cut off.

Results

Experimental data

Figure 3a and c show typical force signals with and without fractures (original and filtered data) at an impact energy of 12.6 J for the fixed and the free configuration respectively. Figure 3b and d show force signals featuring fractures at different energies for the fixed and the free configuration respectively. From Fig. 3a, c, we see that the signal recorded in case of a fracture clearly starts to decrease much earlier. Before the fracture, both signals are identical. Comparison with video images revealed that at the instant, the signal starts to decrease corresponds to the fracture time. The random uncertainty in determining the fracture time from the video images of the

Fig. 2 Impact model and original system of differential equations (DE). Dots over a symbol refer to a derivative with respect to time. The original system (DE) was then reduced to two ordinary differential equations and numerically solved with the initial conditions (IC)

DE:
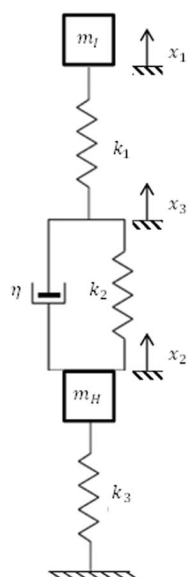
$$m_I \ddot{x}_1 + m_I g + k_1(x_1 - x_3) = 0$$

$$k_1(x_3 - x_1) + k_2(x_3 - x_2) + \eta(\dot{x}_3 - \dot{x}_2) = 0$$

$$m_H \ddot{x}_2 + m_H g + k_3 x_2 + k_2(x_2 - x_3) + \eta(\dot{x}_2 - \dot{x}_3) = 0$$
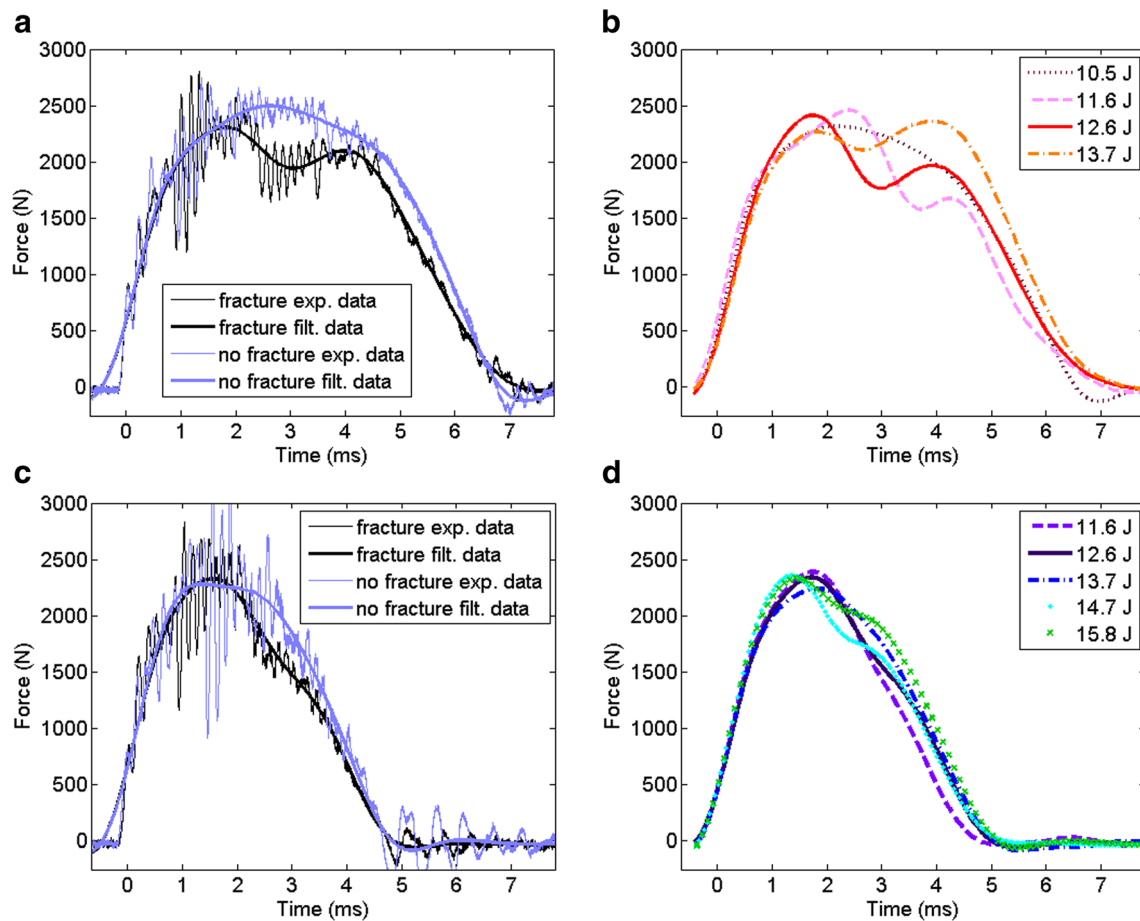
Fig. 3 Force signals at an impact energy of 12.6 J for the fixed (**a**) and the free configuration (**c**). Force signals at different energies featuring fractures for the fixed (**b**) and the free configuration (**d**)

high speed camera was $\pm$ 125 μs. From Fig. 3b, we see that for the fixed configuration, all signals—apart from the one at 10.5 J—have a second peak. This comes from the round shape of the impactor. First, only a small area presses on the head model and a round fracture occurs around this area (an example is illustrated in Fig. 4). The impactor keeps moving after the fracture and the contact area increases. The surrounding intact bone tissue decelerates the impactor further, which leads
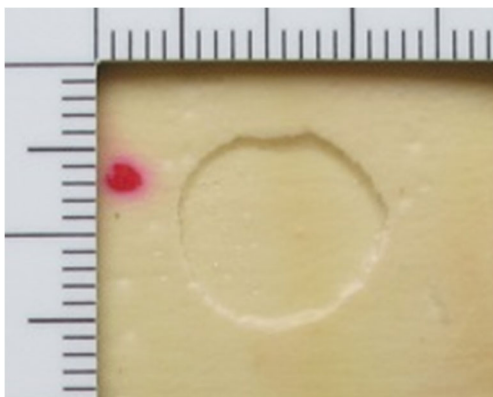

Fig. 4 Example of a fracture at 12.6 J

to the second force peak. In some cases, the amplitude of the second peak was higher than the one of fracture force. This is the case for the signal at 13.7 J in Fig. 3b for which the first peak is at 2267 N and the second one at 2361 N. Note that the shape of the signal recorded at 10.5 J shows no second peak which is typical for signals with no fracture. Nevertheless, we observed exceptions (like the one at 10.5 J) where a fracture occurred on the head model but the force signal had just one peak. Such signals were recorded only in very few cases. In the free configuration, the second peak is much less pronounced looking somehow like knobs (see Fig. 3d). Comparing the signals with the video images, the head model started in this case to move away in direction of the falling impactor. The signal duration in the free configuration is approximately 2 ms shorter than in the fixed one.

From Fig. 5, we see that the fracture forces do not depend on the impact energy used. The mean force for the fixed configuration was (2356 $\pm$ 140) N and for the free configuration, (2307 $\pm$ 120) N. Here, we included the standard deviation of the values of the mean force. Experimental errors are within these intervals. The figure shows that a fracture in the fixed configuration can happen at a much later time than in the free
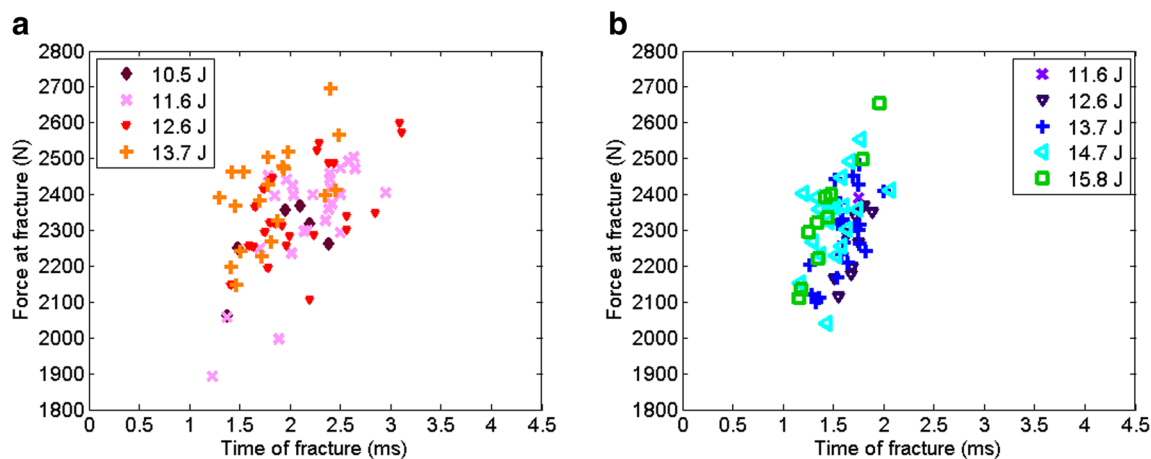
Fig. 5 Fracture force as a function of the time of fracture for the fixed (**a**) and the free configuration (**b**)

configuration. This is confirmed by Fig. 6 where the deformation at fracture is shown. However, no apparent correlation between force and deformation at fracture was found. The mean time of fracture and deformation at fracture are both smaller for the free configuration. Again the reason is that the head model already started to move away reducing the penetration of the impactor and the deformation of the head model. In both configurations, we observed a positive correlation between deformation at fracture and fracture time. Furthermore, an increase of the impact energy leads to an increase in the deformation at fracture. The effect is more pronounced in the fixed configuration. In general, the absorbed energy of the fracture has no obvious dependency on the impact energy. Its mean value is (7.5 ± 0.9) J for the free and (8.4 ± 1.6) J for the fixed configuration. Altogether, the signal data shows that a higher energy impact corresponds to a higher deformation velocity which leads to a shorter mean fracture time as can also be seen, e.g., in Fig. 6 by the increasing slope for higher energy. Analyzing fracture patterns, we found no correlation between the fracture size and the impact energy.

Video images show that in the free configuration, the head had already moved an average distance of 0.7–0.8 mm ($\pm$ 0.3 mm) at the time of fracture and this corresponds to a mean velocity of 1.0–1.2 m/s (± 0.3 m/s). The velocity decreases with increasing impact energy because the fracture occurs earlier and the head has less time to accelerate. For all energies applied, the head motion starts (0.6 ± 0.1) ms after the first contact. A part of the impact energy is transferred to the head before the fracture. Higher impact energy leads to a lower kinetic energy of the head at fracture. The mean kinetic energies of the head are 1.7 J (± 0.6 J) and 2.3 J (± 1 J) for the highest and lowest impact energies respectively. Considering only the influence of the gravity on the head, the mean energies of the head are between 0.3–0.5 mJ at the time of fracture, which are very small compared to the kinetic energies and can therefore be neglected.

Figure 7 shows an example of the impactor penetration into the head model where Fig 7a is an image just before the contact and Fig 7b is an image at the maximum penetration. In Fig. 8, we represent the maximum penetration versus the time of the maximum penetration. For the fixed configuration, the
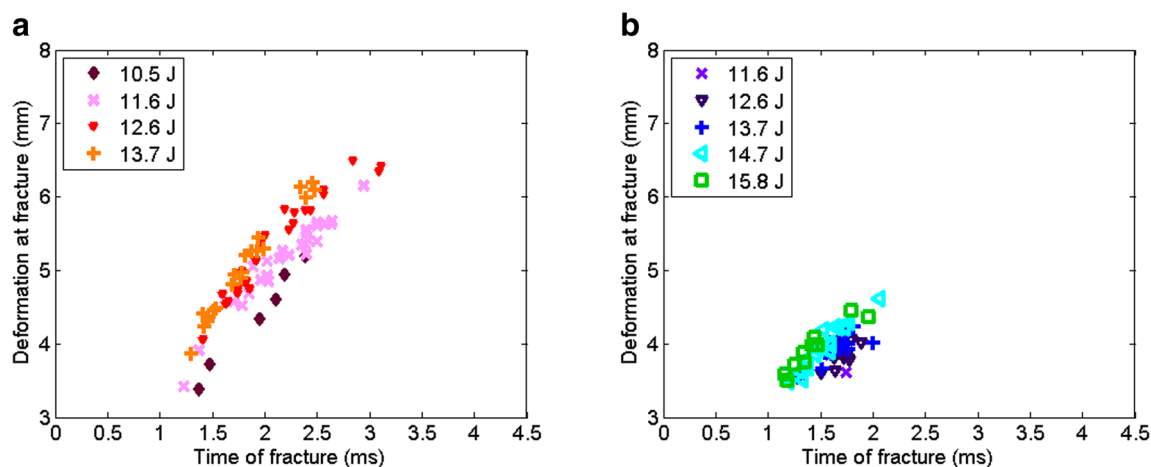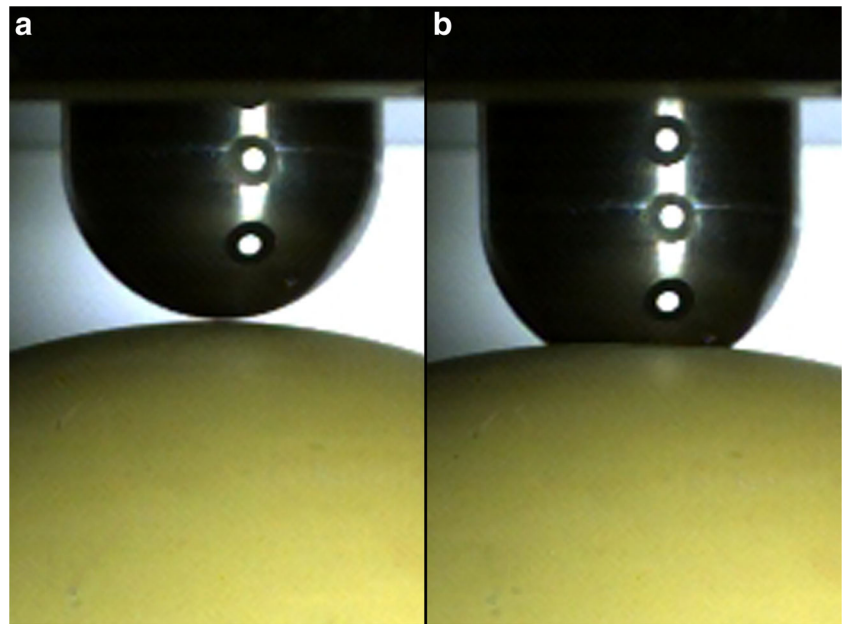

Fig. 6 Deformation at fracture depending on the fracture time for the fixed (**a**) and the free configuration (**b**)

Fig. 7 Impactor penetration. **a** Impactor 0.225 ms before contact. **b** Impactor 3.70 ms after contact at maximum deformation

deformation increases as the impact energy gets higher. This effect is less pronounced for the free configuration.

Figure 9 represents the energy probability distribution for a fracture in both configurations. Black curves are the fits of the cumulative distribution function while vertical gray lines are the 50% threshold value. For the fixed configuration, the 50% threshold corresponds to an energy value of 11.0 J and for the free configuration to a value of 13.6 J.

Mathematical model

Figure 10 displays fits of the mathematical model to experimental data for the fixed (**a**, **b**) and the free configuration (**c**, **d**). Figure 10a and c display the whole signal while in Fig. 10b and d, the signal is cut off after the fracture. The fit of the mathematical model to the signal with the fracture provides a

fracture force of 2407 N (resp. 2402 N) for the fixed (resp. free) configuration. These results are in agreement with (2356 ± 140) N [resp. (2307 ± 120) N] for the fixed [resp. free] configuration, obtained from experimental data (see "Experimental procedure" subsection).

We calculated the mean values of fit parameters for the fixed and the free configuration, with and without fracture. The mathematical model fed by these values showed a reasonable agreement with the experimental data for all cases. Hence, we applied the mathematical model and performed a parameter study to determine the energy threshold for different impactor masses in both configurations. Thereto, a fracture force of 2400 N was chosen. The results are summarized in Table 2. For the free configuration, the energy threshold corresponding to the fracture of the head model gets higher as the impactor mass increases. For the fixed configuration, it
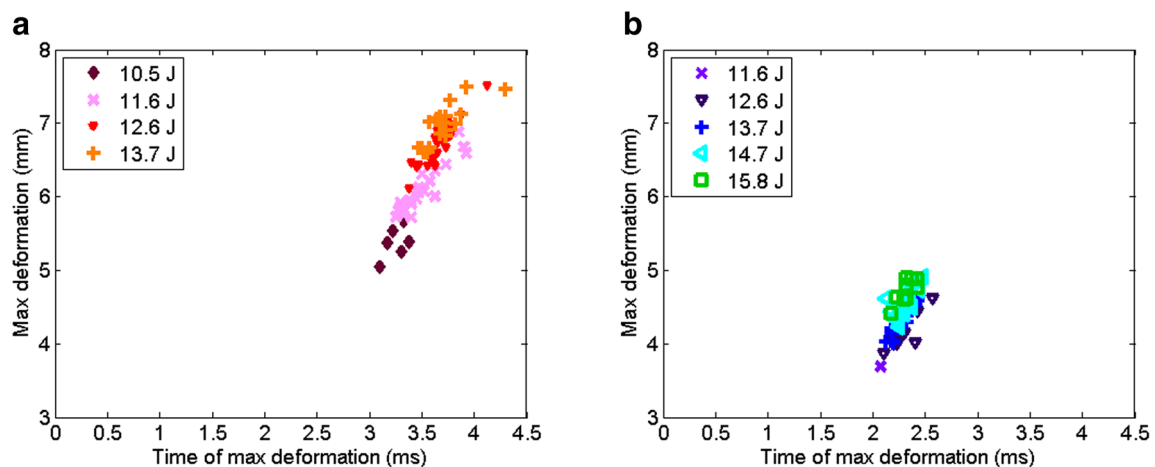

Fig. 8 Maximum deformation as a function of the time of maximum deformation for the fixed (**a**) and the free configuration (**b**)
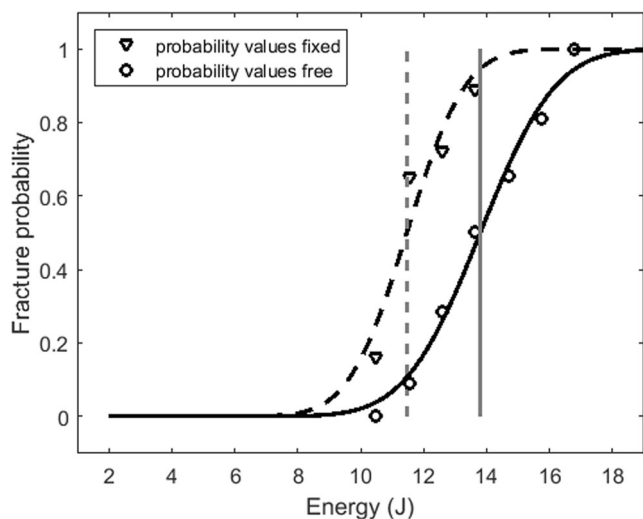
Fig. 9 Fracture probabilities for the fixed and free configuration. The dashed (resp. solid) black curve is the fit of the cumulative distribution for the fixed (resp. free) configuration. The vertical gray lines indicate the 50% threshold values

Table 2 Impactor mass m_I in kg, ratio m_I/m_H, and energy threshold in J needed to fracture the head model for the fixed and the free configuration

m_I (kg)	m_I/m_H	Energy threshold (J)	
		Fixed	Free
1.79	½	9	13.8
2.14	~0.6	8.9	14.7
3.57	1	8.5	18.3
7.14	2	8.1	27.7
10.71	3	7.9	37.7

remains more or less constant. In general, the energy threshold corresponding to the fracture of the head model is lower for the fixed in comparison to free configuration.

Figure 11 shows the mathematical model for impacts at 8.9 J. Black circles indicate fractures in the curves of the force.

Although, the experimental signals would change after the fracture, the tails of the curves are left unchanged as in the case without fracture. For the fixed configuration, only the lightest impactor does not exceed the threshold of 2400 N. At the same energy, there are no fractures for the free configuration.

For the free configuration, the curves of the acceleration of the head are equal but with opposite sign to those of the impactor when $m_I = m_H$, in accordance with Newton's 2nd law. If $m_I < m_H$, the impactor is accelerated more; if $m_I > m_H$, the head is accelerated more. At the same energy, the probability of a fracture is higher for the lighter impactor for the free configuration. At the same energy for the fixed situation, the probability is higher for the heavier impactors.
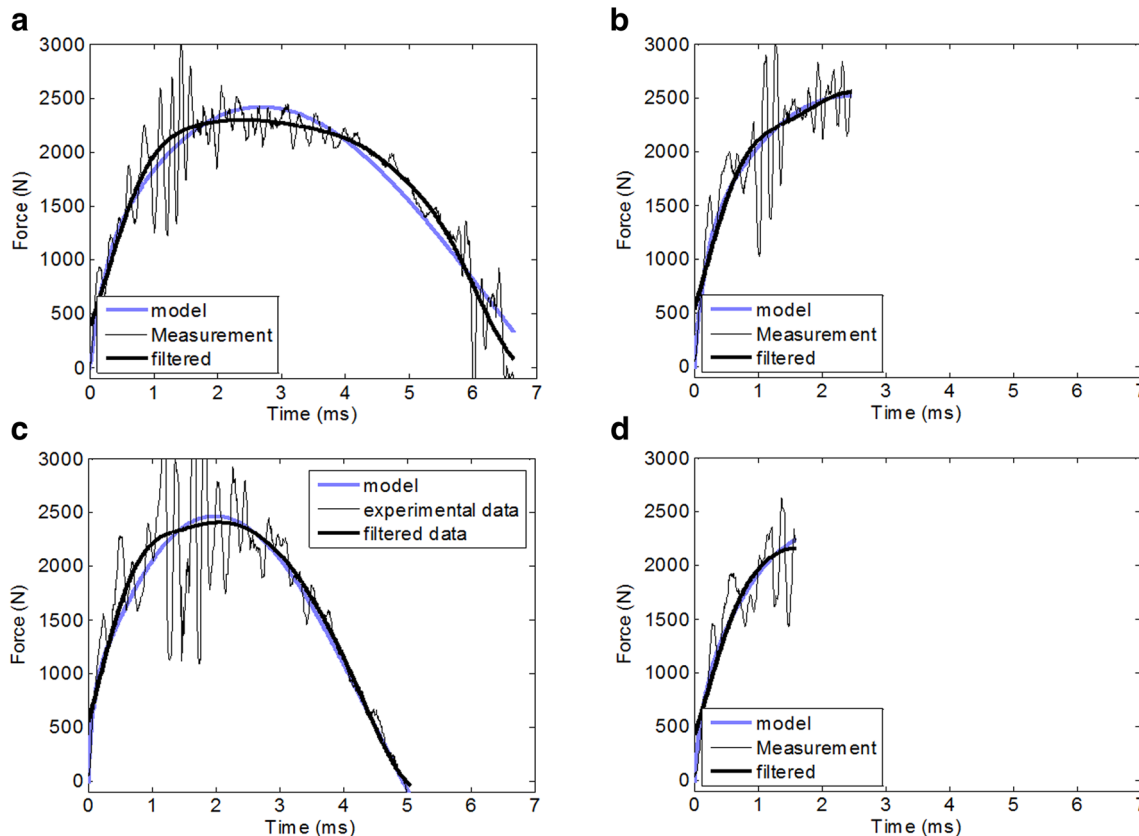

Fig. 10 Fits of the mathematical model to experimental data for the fixed (**a**, **b**) and the free (**c**, **d**) configuration. In **a** and **b**, no fracture occurred. In **b** and **d**, the signal is cut off after the fracture. Examples correspond to an impact energy of 11.55 J
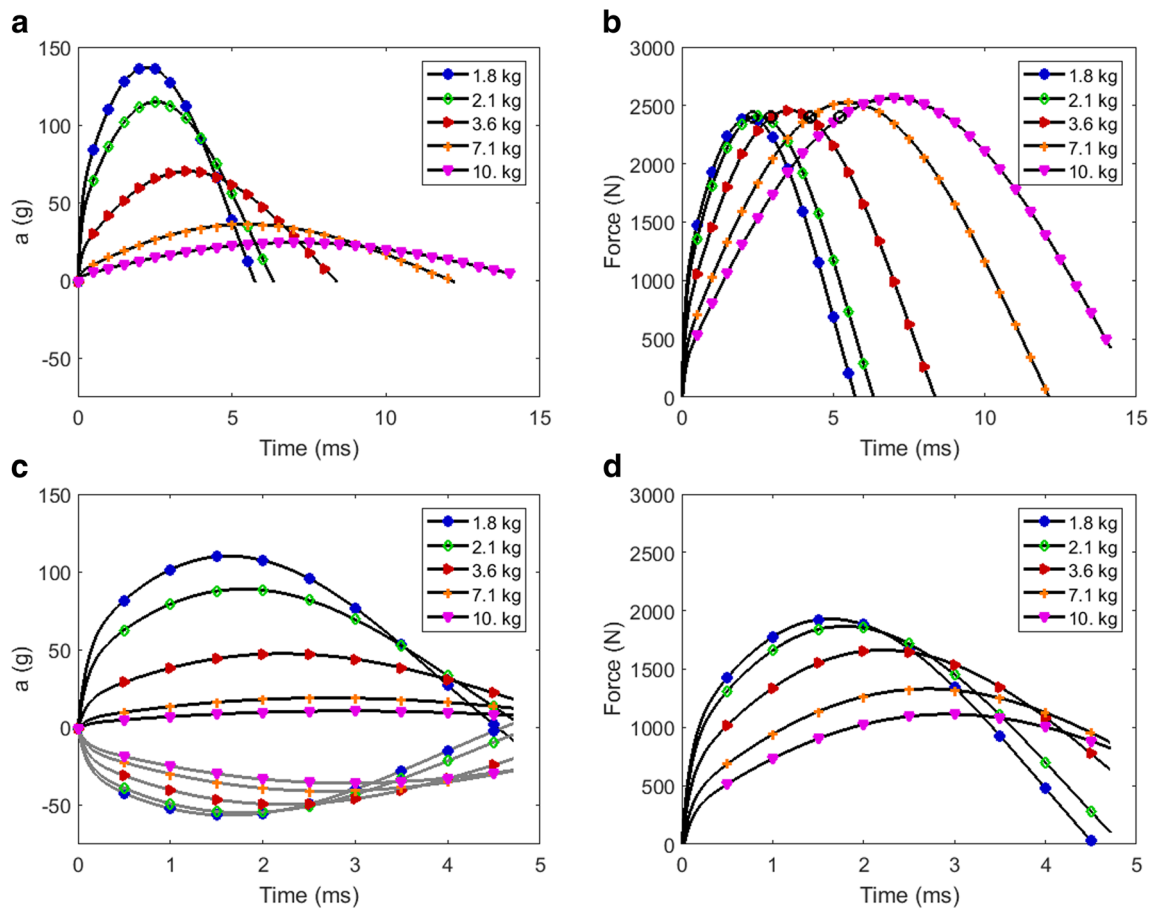
Fig. 11 Mathematical model for impacts at an energy of 8.9 J with different masses. Curves of acceleration (**a**) and force (**b**) for the fixed configuration. Curves of acceleration (**c**) and force of the impactor (**d**) for the free configuration. Note that their time axes are chosen shorter for clarity reasons. Black circles indicate fractures. In **c**, the black lines refer to the impactor while the gray ones do to the head. The force of the head is not represented in **d** as it is equal but with opposite sign to that of the impactor

Discussion

Although our head model cannot be quantitatively compared to real skulls, its qualitative behavior shows a very good agreement [15, 18, 19]. In our experiments, we observed a difference (yet a small one) in the energy thresholds (i.e., approx. 2.6 J) between a head placed on a hard surface and one allowed to freely move. If considering the actual hitting energies of some instruments used in assaults—ranging from 33 J for female hitters with a wrench to 167 J for male hitters with a spade [22, 23], this difference seems to be negligible.

Comparing the forces measured with our head models with the forces found for real skulls listed in the introduction [5–7, 10, 11, 14] reveals that our results are at the very low end of the scale. Since the qualitative behavior shows a good agreement [15, 18, 19], our results should be scalable and therefore allow us to estimate the influence of the boundary conditions on a real skull. Schneider et al. [10] reported energy values necessary to fracture human skulls with intact scalp. Fractures of the frontal bone start at 37 J and clinically significant fractures at 47 J. For the temporo-parietal bone, they start at 16 J

and clinically significant fractures at 21 J. In our experiments, we did not use a skin simulant.

Furthermore, because of the great variability of biological tissue, real skulls present force thresholds for fracture varying from subject to subject. It can be assumed that the energy thresholds vary accordingly and that its effect is well larger than 2.6 J. This means that in a forensic case, the two situations most probably could not be distinguished.

Interestingly, we found no correlation between the size of the fracture and the impact energy. The reason might be that we used relatively small changes in the impact energies. Perhaps, larger changes would have led to a correlation.

This study focused on bone fractures disregarding effects on the underlying tissue. The maximum deformation (or maximum penetration) of the impactor in the head however influences the damage caused to the brain. Depending on the impact energy, we found here a difference in the maximum deformation of about 1.0–2.5 mm between the fixed and the free configuration. This result might be useful to distinguish in which situation a brain damage occurred. However, further studies on brain injuries are needed to deepen this aspect.

Verschueren and Delye et al. [5, 6] concluded that the probability of fracture is not influenced whether the head is fixed or can freely move. On the contrary, we found that even a small motion of less than 1 mm has an effect. This discrepancy might be explained by the fact that we used a spherical head model whereas Verschueren and Delye et al. [5, 6] employed real human heads with varying mechanical properties.

These inter individual differences between human skulls might also explain the differences in the fracture force for free and fixed boundary conditions presented by Kroman et al. [9]. However, their fracture times are well in agreement with our results. Schneider et al. [10] and Nahum et al. [11] claimed (without presenting any results) that the impact force increases if the head is placed on a rigid surface, a trend not supported by our study.

By means of a numerical simulation, Ruan et al. [12, 13] observed a difference in the pressure response inside the head between a freely moving head and a head in a fixed condition. Although, we did not measure the pressure inside the model, these results are in agreement with the accelerations of the head measured in this study.

Our mathematical model fits the data rather well, but it cannot reproduce the exact energy thresholds. It rather can be applied to study tendencies for both configurations by varying the impactor mass m_I. From Fig. 11c, we see that at the same energy the head is accelerated if m_I becomes larger. This leads to a lower maximum force as m_I becomes larger (see Fig.11d). Hence, more energy is needed to reach the same fracture force threshold. Altogether, as m_I becomes larger, the difference between the energy thresholds of the two configurations increases. This means that in a forensic case in principle for heavy objects, the two configurations can be distinguished.

For an object with a small mass, the boundary condition does not influence the fracture probability. For an object with a high mass, the boundary condition needs however to be taken into consideration.

Limitations

The main limitation of this study is the use of a synthetic material filled with gelatin, whose time-dependent and post-yield material properties differ from human skull bone and brain. In particular, the stiffness and damping parameters obtained with the mathematical model are presumably different for a real head. Nevertheless, the use of a bone and brain simulant has the important benefit of being highly reproducible. A further limitation is the use of just one kind of impactor. Further experiments are needed to study the influence of the shape and mass of the impactor.

Conclusion

The fracture threshold of a head model was determined for a fixed and a free configuration. It turned out that the fracture force for both configurations were the same, whereas the energy threshold for head fracture was 2.6 J higher for the free configuration. This difference seems to be negligible if compared to the effect of varying mechanical properties of real human heads.

The influence of the impactor mass was investigated by means of a mathematical model. The energy threshold for the fixed configuration decreases slightly with increasing impactor mass whereas for the free configuration, it increases with a larger impactor mass. These results reveal that boundary conditions must be considered if heavy weapons have been used.

Compliance with ethical standards

Conflict of interest   The authors declare that they have no conflict of interest.

References

1. Park J, Son H (2017) Weapon use in Korean homicide: differences between homicides involving sharp and blunt instruments. J Forensic Sci 63:1134–1137. https://doi.org/10.1111/1556-4029.13673

2. Ambade VN, Godbole HV (2006) Comparison of wound patterns in homicide by sharp and blunt force. Forensic Sci Int 156(2–3):166–170. https://doi.org/10.1016/j.forsciint.2004.12.027

3. Stiell IG, Wells GA, Vandemheen K, Clement C, Lesiuk H, Laupacis A, McKnight RD, Verbeek R, Brison R, Cass D, Eisenhauer ME, Greenberg G, Worthington J (2001) The Canadian CT head rule for patients with minor head injury. Lancet 357(9266):1391–1396

4. Yoganandan N, Zhang J, Pintar F (2004) Force and acceleration corridors from lateral head impact. Traffic Inj Prev 5(4):368–373. https://doi.org/10.1080/15389580490510336

5. Verschueren P, Delye H, Depreitere B, Van Lierde C, Haex B, Berckmans D, Verpoest I, Goffin J, Vander Sloten J, Van der Perre G (2007) A new test set-up for skull fracture characterisation. J Biomech 40(15):3389–3396. https://doi.org/10.1016/j.jbiomech.2007.05.018

6. Delye H, Verschueren P, Depreitere B, Verpoest I, Berckmans D, Vander Sloten J, Van Der Perre G, Goffin J (2007) Biomechanics of frontal skull fracture. J Neurotrauma 24(10):1576–1586. https://doi.org/10.1089/neu.2007.0283

7. Mole CG, Heyns M, Cloete T (2015) How hard is hard enough? An investigation of the force associated with lateral blunt force trauma to the porcine cranium. Legal Med 17(1):1–8. https://doi.org/10.1016/j.legalmed.2014.07.008

8. Viano DC, Bir C, Walilko T, Sherman D (2004) Ballistic impact to the forehead, zygoma, and mandible: comparison of human and frangible dummy face biomechanics. J Trauma 56(6):1305–1311

9. Kroman A, Kress T, Porta D (2011) Fracture propagation in the human cranium: a re-testing of popular theories. Clin Anat 24(3):309–318. https://doi.org/10.1002/ca.21129

10. Schneider D, Nahum A (1972)Impact Studies of Facial Bones and Skull. In: 16th Stapp Car Crash Conference, 1972/02/01/ 1972. https://doi.org/10.4271/720965

11. Nahum AM, Gatts JD, Gadd CW, Danforth J (1968) Impact Tolerance of the Skull and Face. 12th Stapp Car Crash Conference Proceedings. SAE No. 680785, No. 680785 edn. SAE International, Warrendale, PA. https://doi.org/10.4271/680785

12. Ruan JS, Khalil T, King AI (1991) Human head dynamic response to side impact by finite element modeling. J Biomech Eng 113(3): 276–283

13. Ruan JS, Khalil T, King AI (1994) Dynamic response of the human head to impact by three-dimensional finite element analysis. J Biomech Eng 116(1):44–50

14. Raymond D, Van Ee C, Crawford G, Bir C (2009) Tolerance of the skull to blunt ballistic temporo-parietal impact. J Biomech 42(15): 2479–2485. https://doi.org/10.1016/j.jbiomech.2009.07.018

15. Thali MJ, Kneubuehl BP, Dirnhofer R (2002) A "skin–skull–brain model" for the biomechanical reconstruction of blunt forces to the human head. Forensic Sci Int 125(2):195–200. https://doi.org/10.1016/S0379-0738(01)00639-9

16. Thali MJ, Kneubuehl BP, Zollinger U, Dirnhofer R (2002) The "skin–skull–brain model": a new instrument for the study of gunshot effects. Forensic Sci Int 125(2):178–189. https://doi.org/10.1016/S0379-0738(01)00637-5

17. Kneubuehl BP, Coupland R, Rothschild M (2011) Wound Ballistics: Basics and Applications, 1st edn. Springer-Verlag Berlin Heidelberg, Berlin Heidelberg. https://doi.org/10.1007/978-3-642-20356-5

18. Franckenberg S, Nyffeler RW, Siegenthaler L, Kneubuehl BP, Bolliger SA, Thali MJ, Ross SG, Vonlanthen B (2013) Three cases of humeral shaft fracture during police arrest —biomechanical aspects and reconstruction of events. J Forensic Radiol Imaging 1(3): 112–118. https://doi.org/10.1016/j.jofri.2013.05.006

19. Smith MJ, James S, Pover T, Ball N, Barnetson V, Foster B, Guy C, Rickman J, Walton V (2015) Fantastic plastic? Experimental evaluation of polyurethane bone substitutes as proxies for human bone in trauma simulations. Leg Med (Tokyo) 17(5):427–435. https://doi.org/10.1016/j.legalmed.2015.06.007

20. Raymond DE, Bir CA (2015) A biomechanical evaluation of skull-brain surrogates to blunt high-rate impacts to postmortem human subjects. J Forensic Sci 60(2):370–373. https://doi.org/10.1111/1556-4029.12693

21. Cronin DS, Falzon C (2011) Characterization of 10% ballistic gelatin to evaluate temperature, aging and strain rate effects. Exp Mech 51(7):1197–1206. https://doi.org/10.1007/s11340-010-9438-z

22. Sprenger FD, Siegenthaler L, Kneubuehl BP, Jackowski C (2015) The influence of striking object characteristics on the impact energy. Int J Legal Med 130:835–844. https://doi.org/10.1007/s00414-015-1268-1

23. Siegenthaler L, Sprenger FD, Kneubuehl BP, Jackowski C (2018) Impact energy of everyday items used for assault. Int J Legal Med 132(1):211–217. https://doi.org/10.1007/s00414-017-1689-0